Blends of Poly(vinyl chloride) with Acrylonitrile–Chlorinated Polyethylene–Styrene Copolymer. II. Mechanical Properties

ZHIKAI ZHONG,[1] SIXUN ZHENG,[1] KEJIA YANG,[2] QIPENG GUO[1]

[1] Department of Polymer Science and Engineering, University of Science and Technology of China, Hefei 230026

[2] Anhui Research Institute of Chemical Technology, Hefei 230041, People's Republic of China

Received 29 May 1996; accepted 20 September 1996

ABSTRACT: Blends of poly(vinyl chloride) (PVC) and acrylonitrile–chlorinated polyethylene–styrene (ACS) graft copolymer were prepared by melt blending. Mechanical properties were studied by the use of dynamic mechanical analysis (DMA), impact tests, tensile tests, and scanning electron microscopy (SEM). The DMA study showed that PVC is immiscible with chlorinated polyethylene in ACS but partially miscible with poly(styrene-*co*-acrylonitrile) (25% acrylonitrile content) in ACS. Mechanical property tests showed that there is a significant increase in the impact strength while other good mechanical properties of PVC such as high modulus and high strength remain. SEM observations supported the results of the mechanical properties studies. © 1997 John Wiley & Sons, Inc. J Appl Polym Sci **64:** 399–405, 1997

Key words: poly(vinyl chloride); ACS copolymer; polymer blends; mechanical properties

INTRODUCTION

During the past decades, considerable attention has been devoted to the modification of poly(vinyl chloride) (PVC), including plasticization, enhancement of impact strength, increase of heat distortion temperature, and improvement of processibility.[1–5] Usually, improvement of the impact strength of rigid PVC can be reached by the addition of polymeric modifiers such as chlorinated polyethylene (CPE),[6] ethylene–vinyl acetate copolymers,[7] nitrile rubbers,[8] and acrylonitrile–butadiene–styrene copolymer (ABS) or methylmethacrylate–butadiene–styrene copolymer (MBS).[9–12] Of these impact modifiers, ABS has received special attention because it combines the impact strength of polybutadiene rubber and the tensile strength and heat stability of the styrene–acrylonitrile copolymer (SAN) matrix,[13–15] which are also imparted in PVC/ABS blends. PVC/ABS blends have been shown to have a significant increase in impact strength and heat distortion temperature.[9–11]

Acrylonitrile–chlorinated polyethylene–styrene copolymer (ACS) is a graft copolymer which is very similar to ABS, and hence, it is expected to be an impact modifier of PVC. In ACS, the rubbery phase is made of chlorinated polyethylene, which constitutes the main polymer chain; the glassy phase is made of styrene and acrylonitrile, which graft onto chlorinated polyethylene. Furthermore, ACS enjoys good weather resistance, because there is no unsaturated link in its chains, and good fire resistance, because it contains CPE. The corrosion resistance of ACS is also superior to that of ABS. Thus, compared with ABS, the use of ACS as an impact modifier of PVC may have several significant advantages. Actually, some patents

Correspondence to: Q. Guo.

 CCC 0021-8995/97/020399-07

have involved the blends of ACS with PVC.[16,17] However, to our knowledge, no systematical investigation concerning miscibility and morphology, as well as the properties of the PVC/ACS blends, has been reported in the literature.

In a previous article,[18] we reported the results of our investigation on the miscibility, phase behavior, and thermal stability of PVC/ACS blends. By means of differential scanning calorimetry (DSC) and thermogravimetric analysis, we found that PVC is immiscible with CPE in ACS, whereas it is partially miscible with SAN in ACS. The PVC/ACS blends exhibit a three-phase structure, and ACS can significantly improve the thermal stability of PVC. In this article, we present further the results of our research on the mechanical properties of the PVC/ACS blends.

EXPERIMENTAL

Materials and Preparation of Blends

The PVC resin (PVC S-700) was purchased from Qilu Petrochemical Co., Zipou, Shandong, China; it had an average degree of polymerization of 650–750. The ACS, with a melting index of 0.88 g/min (190°C, 10.8 kg), was provided by Anhui Research Institute of Chemical Technology, Hefei, Anhui, China. The styrene/acrylonitrile (St/AN) in the ACS was 3/1 in terms of weight ratio, i.e., the SAN in the ACS had 25 wt % AN content. The ACS was prepared by grafting St and AN onto CPE, and the content of CPE in the ACS was 27 wt %. The CPE was obtained from Wuhu Chemicals Factory, Anhui, China; it was rubbery type and had 36 wt % chlorine content. Tribasic lead sulfate and dibasic lead stearate, supplied by Wenzhou Plastics Additives Factory, Wenzhou, Zhejiang, China, were used as heat stabilizers for PVC.

The PVC/ACS blends were prepared by melt mixing. The preweighed mixtures of PVC and ACS, together with stabilizers, were first mixed in a high-speed mixer for 30 min at room temperature and then milled for 5 min on a two-roll mill at 160°C. The samples thus obtained were molded into sheets (about 4 mm thick) with a hot press molding machine at 170°C and 100 atm for 5 min. The blend compositions studied were 100/0, 80/20, 60/40, 40/60, 20/80, and 0/100 PVC/ACS in terms of weight ratio. In order to prevent possible degradation, 1.5 wt % stabilizers were added to the blends.

Dynamic Mechanical Measurements

Dynamic mechanical measurements were carried out on a Rheovibron Model DDV-III-EA dynamic viscoelastometer (Toyo Baldwin Co., Japan). The frequency used was 35 Hz, and the heating rate was 3.0°C/min. The specimen dimension was 6.0 $\times$ 0.4 $\times$ 0.2 cm^3.

Izod Impact Tests

Notched Izod impact tests was done on an AFS/MK3-654S/000 Izod impact tester (CEAST Co., Germany) at 20°C, according to ASTM D256 standard. A minimum of five specimens with a notched angle of 45° were tested in all cases.

Tensile Tests

Tensile tests were carried out on an AG-5000A testing machine at 20°C. Standard dumbbell specimens (ASTM D638) with 2.5 $\times$ 0.6 $\times$ 0.4 cm^3 neck were used. A minimum of five specimens were tested in all cases. The crosshead speed was 5 mm/min, corresponding to a relative strain rate of 0.2/min.

Morphological Observation

To investigate the morphology of PVC/ACS blends, the specimens were fractured under cryogenic conditions with liquid nitrogen. A Hitachi X-60 scanning electron microscope (SEM) was used for observation, before which, the surfaces were coated with thin layers of gold of 200 Å.

RESULTS AND DISCUSSION

Dynamic Mechanical Properties

Pure PVC

The dynamic mechanical properties of PVC have been studied intensively, and a general review has been made in references 19–23. Our results, shown in Figure 1, are similar to those that have been reported in the literature. The loss modulus (E'') versus temperature (T) curve exhibits two relaxation peaks. The low-temperature β-relaxation peak is at $-50 \sim 0$°C, and the high-temperature α-relaxation peak is at ca. 109°C. Because the storage modulus (E') decreases sharply at ca. 109°C, indicating that the material becomes soft at that temperature, the α-relaxation was attrib-

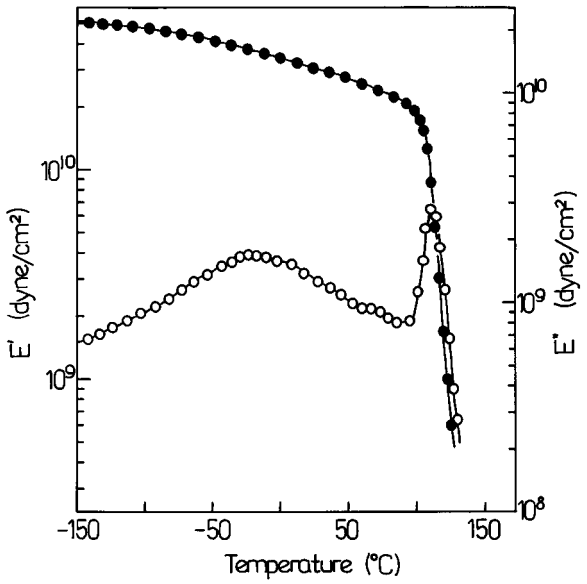

Figure 1 Dynamic viscoelastic properties of PVC: (●) storage modulus E', (○) loss modulus E''.

uted to the transition from the glassy to the viscoelastic state. The low-temperature β-relaxation peak was attributed to a twisting motion of a chain segment about its long axis, i.e., segment flipping, by Havriliak and Shortridge.[22]

Pure ACS

The dynamic mechanical properties of ACS are shown in Figure 2. The E'' versus T curve shows five well-defined relaxation peaks at about 136, 70, −11, −50, and −110°C, denoted by α-, β-, γ-, δ-, and ϵ-relaxations, respectively. It can be seen that the α-relaxation and γ-relaxation are very sharp and are due to micro-Brownian motion of the polymer chains. They correspond to the glass-rubber transition of CPE and SAN in ACS, respectively. For β-, δ-, and ϵ-relaxation, their origins are not known at present, and a detailed study is in progress.

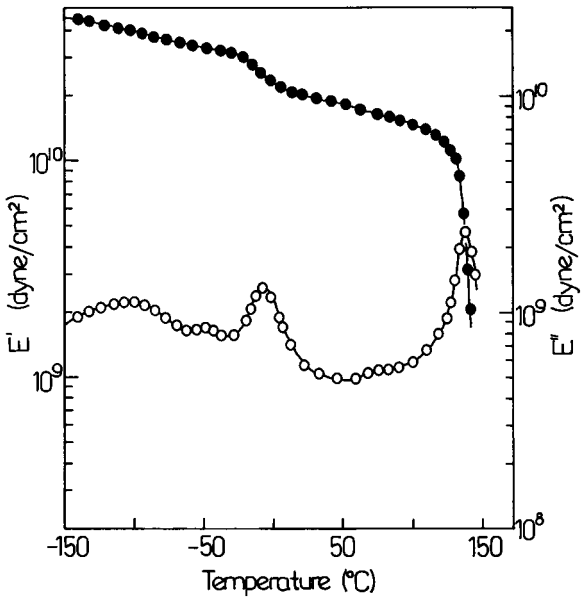

Figure 2 Dynamic viscoelastic properties of ACS: (●) storage modulus E', (○) loss modulus E''.

The Blends

Figure 3 illustrates the temperature dependence of E'' for the PVC/ACS blends. The E'' versus T curves of all of the blends show a sharp relaxation peak at about −11°C. With an increase of ACS content, this relaxation peak becomes sharper and sharper; however, its location remains almost unchanged. This relaxation peak is due to the α-relaxation (glass transition) of the CPE component in the blends, which overlaps with the β-relaxation peak of PVC. From Figure 3, it can also be seen that blending with ACS suppresses the β-relaxation of PVC and enhances the α-relaxation of CPE, in particular, when the content of ACS is more than 20 wt %. This may be the reason for the sharp increase of the impact strength of the blends beyond 20 wt % ACS, as discussed be-

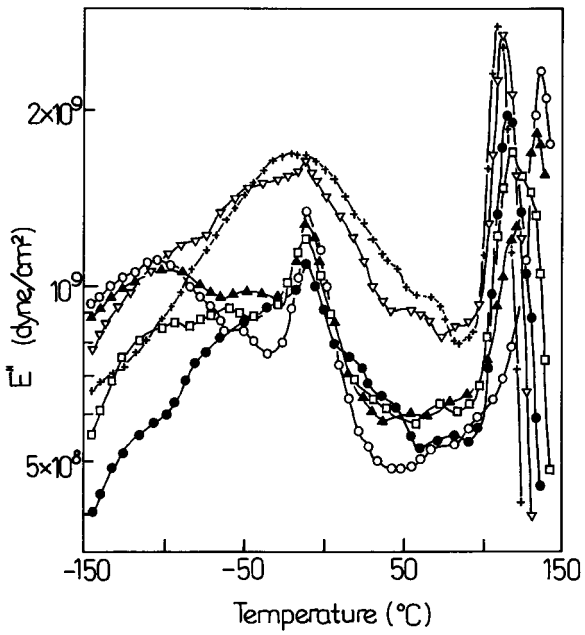

Figure 3 Temperature dependence of loss modulus E'' of PVC/ACS blends. PVC/ACS: (+) 100/0, (▽) 80/20, (●) 60/40, (□) 40/60, (▲) 20/80, (○) 0/100.

Table I Glass Transition Temperature of the PVC/ACS Blends

PVC/ACS	T_g (°C) CPE Phase	PVC-Rich Phase	SAN-Rich Phase
100/0		109.0	
80/20	−10.9	112.1	124.1
60/40	−10.8	115.0	127.1
40/60	−10.9	118.0	130.1
20/80	−10.9	118.1	133.0
0/100	−10.8		136.0

low. Above 80°C, the E'' versus T curves exhibit two relaxation peaks. The low-temperature relaxation peak shifts to high temperature and its height decreases with increasing ACS content in the blend, whereas the high-temperature relaxation peak shifts to low temperature and its height decreases with decreasing ACS content in the blend. The low-temperature relaxation peak corresponds to the glass transition of the PVC-rich phase, and the high-temperature relaxation peak is due to the glass transition of the SAN-rich phase. The T_g data obtained from Figure 3 are listed in Table I and are plotted in Figure 4 as a function of blend composition. From Figure 4, it can be seen clearly that the T_g of the CPE phase is independent of the blend composition, whereas the T_g of the PVC-rich phase increases with an increase of ACS content and, hence, SAN content; the T_g of the SAN-rich phase decreases with an increase of PVC content. These results are consistent with our previous DSC study on this system[18] and suggest that PVC is immiscible with CPE in ACS but is partially miscible with SAN in ACS; also, the PVC/ACS blends exhibit a three-phase structure: the CPE phase, the PVC-rich phase, and the SAN-rich phase.

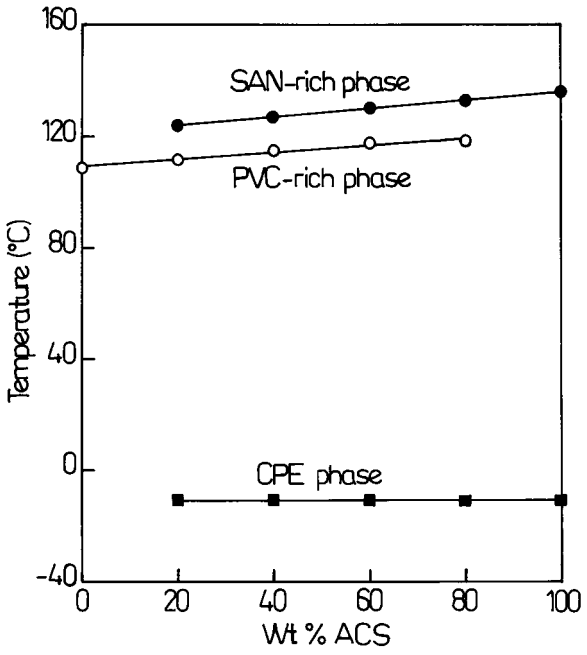

Figure 4 Glass transition temperatures of PVC/ACS blends.

Table II Mechanical Properties of the PVC/ACS Blends

PVC/ACS	Impact Strength (J/m)	E (GPa)	σ_y (MPa)	σ_b (MPa)	ϵ_b (%)
100/0	31.8	2.37	56.5	47.8	125.0
80/20	32.3	2.25	50.0	33.6	144.0
60/40	94.6	2.12	48.7	31.0	80.0
40/60	190.8	2.02	46.1	28.3	20.0
20/80	233.5	1.74	36.8	24.9	60.0
0/100	237.8	1.49	29.3	21.6	46.7

Izod Impact Strength

The incorporation of ACS in PVC results in a considerable increase in notched Izod impact

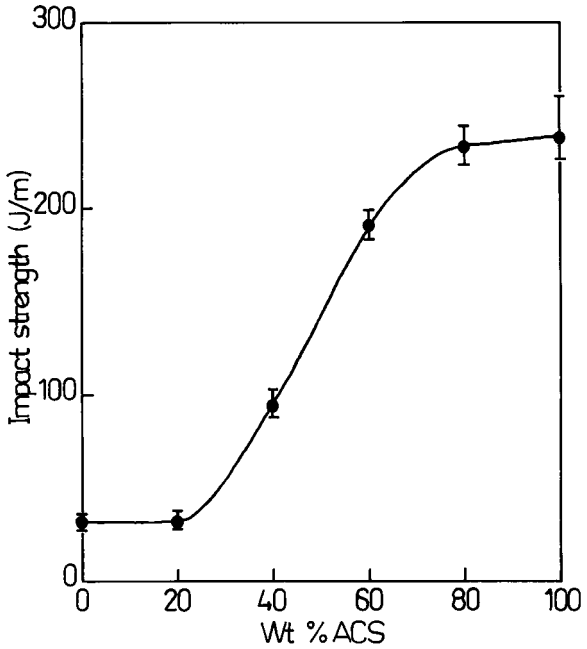

Figure 5 Composition dependence of Izod impact strength at room temperature (20°C) for PVC/ACS blends.

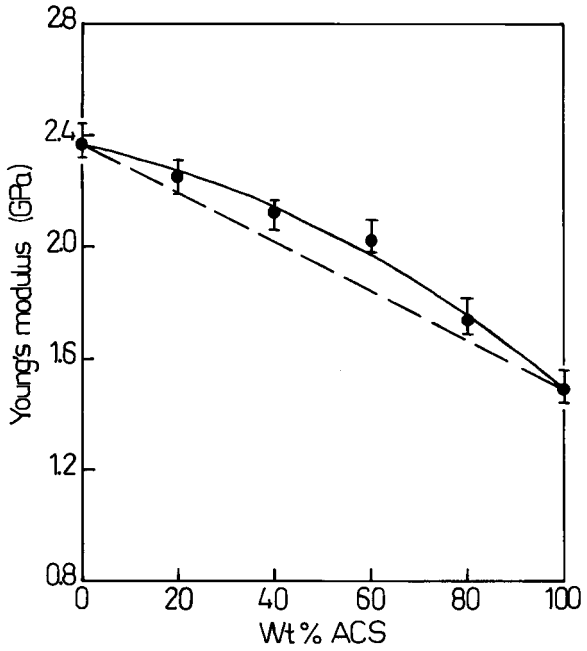

Figure 6 Dependence of Young's modulus at room temperature (20°C) on composition for PVC/ACS blends.

strength over that of pure PVC (Fig. 5 and Table II). It can be seen from Figure 5 that the impact strength increases monotonically with increasing ACS content in the blend, and the variation of the impact strength on composition exhibits an S-shape. The impact strength remains almost constant with ACS content up to 20 wt % in the blend; then, it begins to increase greatly with increasing ACS content. However, the impact strength remains essentially invariant when the content of ACS is beyond 80 wt %. It is interesting to point out that the macroscopic fractured surface of the impact specimen was smooth for pure PVC. However, the fractured surface became more and more coarse with the addition of ACS content in the blend, and some characteristics of ductile fracture clearly appeared at high ACS content.

In ACS, CPE rubber constitutes the main polymeric chain to which St and AN are grafted. The CPE contributes to the toughness of the materials, which is similar to the PVC/ABS case.[11] With increasing ACS content, the CPE content in the blend also increases and the blends will have more rubbery CPE dispersed in the rigid and glassy matrix. Thus, the impact strength of the blends improves with the incorporation of ACS. As we have mentioned above, the α-relaxation of CPE, which is below zero temperature, becomes more and more significant with the increase of ACS content, and there is a sharp change in the range of 20–40 wt % ACS. Therefore, the impact strength increases greatly beyond 20 wt % ACS. The interaction between the phases in the PVC/ACS blends may also contribute to the improvement of the impact strength of the blends, and this will be seen further by SEM observation.

Tensile Properties

The common stress–strain behavior was obtained for PVC, ACS, and their blends. The obvious yield and neck formation are observed on the stress-strain curve, which shows that PVC, ACS, and their blends are ductile materials at the strain rate of 0.2/min and room temperature (20°C). Young's moduli (E) of PVC, ACS, and their blends were calculated from the initial slopes of the stress-strain curves (Table II). In Figure 6, the Young's modulus is plotted against the blend composition. It can be seen, first, that the Young's modulus decreases with increasing ACS content in the blends, which is due to the lower modulus of ACS. Second, the Young's modulus shows positive deviations from simple additivity over the entire composition range. These positive deviations suggest that there is enough interaction between the components to retard its internal mobility significantly.[24–27]

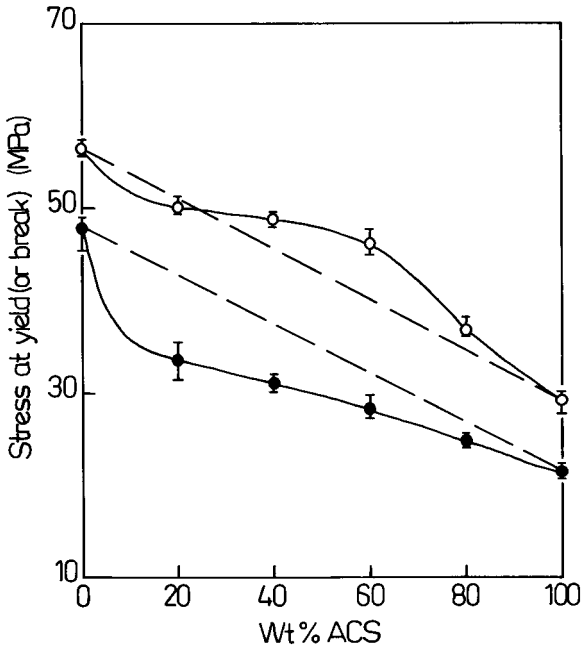

Figure 7 Composition dependence of strength at room temperature (20°C) for PVC/ACS blends: (○) stress at yield, (●) stress at break.

The properties at high deformation are summarized in Table II and illustrated in Figures 7 and 8 by the stress at yield (σ_y), the stress at break (σ_b), and the elongation at break (ϵ_b). In Figure 7, the open circles represent stress at yield and the solid circles represent stress at break. From Figure 7, it can be seen that, first, the stress at yield is greater than the stress at break for the specimens with the same composition. Second, when ACS was incorporated in PVC, there is a decrease in both stress at yield and stress at break, attributing to the relatively poor mechanical properties of ACS (Table II). Third, the curve of the stress at yield versus the blend composition shows essentially positive deviations from simple additivity, except for the 80/20 PVC/ACS blend, for which the yield stress falls below the corresponding weight-average value. The essentially positive deviations indicate that there is enough interaction between the components. However, the curve of the stress at break versus the blend composition exhibits negative deviations from the simple additivity. This is because yield occurred at relatively low strain and was dominated by the continuous phase, whereas fracture occurred at high strain and was considered to be flaw controlled.

It is interesting to see that the elongation at break exhibits a very complicated shape (Fig. 8). At some blend compositions, the elongation at break exceeds the corresponding weight-average value, whereas it falls below at other blend compositions. Similar results were observed in chlorinated polyether/poly(vinyl acetate) blends.[28] The elongation at break reflects, to some extent, the mobility of macromolecular chains. The extremely large elongation at break of the 80/20 PVC/ACS blend, which is even larger than that of both pure components, perhaps indicates the high mobility of macromolecular chains in this blend.

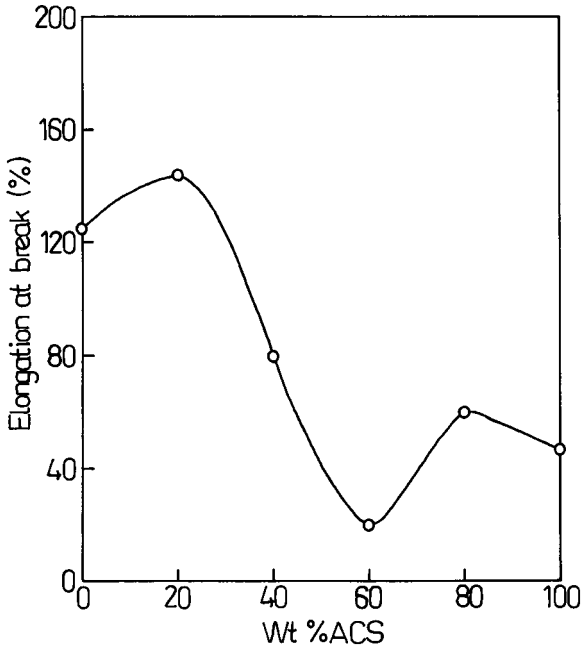

Figure 8 Composition dependence of elongation at break at room temperature (20°C) for PVC/ACS blends.

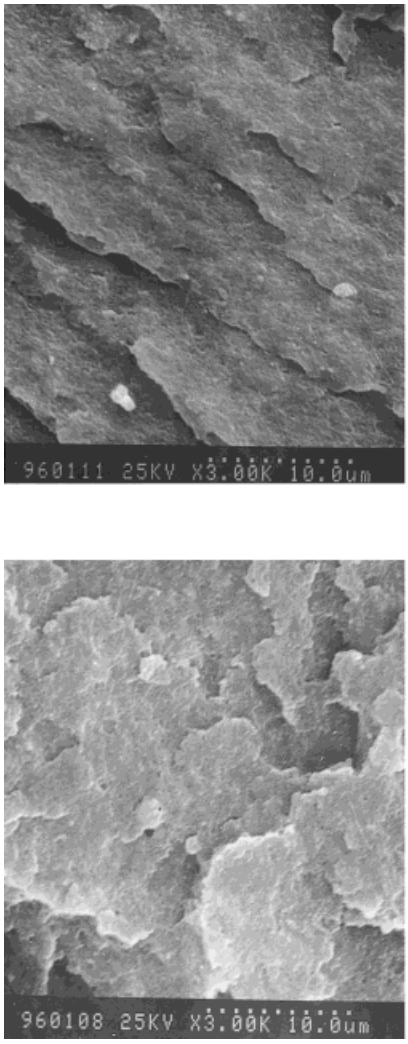

Figure 9 Scanning electron micrographs of fractured surfaces of (a) 80/20 and (b) 20/80 PVC/ACS blends.

Morphology

Scanning electron microscopy (SEM) studies were carried out to support the results obtained by studying the mechanical properties of PVC/ACS blends. The specimens were fractured under cryogenic conditions with liquid nitrogen. The

SEM photographs of the fractured surface of the 80/20 and 20/80 PVC/ACS blends are shown in Figure 9(a,b), respectively. From Figure 9, it can be seen that small spherical CPE domains were dispersed on a fine scale in the continuous phase. The SEM photographs also show what appear to be vacant holes from which the CPE phase was pulled out. The average domain size is less than 0.3 μm in diameter, with the largest of these domains being ca. 0.5 μm. It can also be seen from the figure that the interfacial adhesion between the phases in the PVC/ACS blends is rather good, and this is consistent with the results of the tensile properties. In addition, the fractured surface of the 80/20 PVC/ACS blend is relatively smooth [Fig. 9(a)], indicating that the fracture occurred in a macroscopically brittle manner. However, the fractured surface of the 20/80 PVC/ACS blend is rather coarse [Fig. 9(b)] and exhibits some characteristics of ductile fracture. These results are consistent with the increasing impact strength as the ACS is incorporated into PVC.

CONCLUSIONS

The results presented in this article show that PVC is immiscible with CPE in ACS but is partially miscible with SAN in ACS. The incorporation of ACS in PVC results in a considerable increase in the impact strength over that of pure PVC, and at the same time, the materials essentially retain other good mechanical properties of PVC such as high modulus and high strength. ACS can be used as an impact modifier of PVC. The results of the mechanical properties of the PVC/ACS blends were supported by SEM observations.

The financial support from the Presidential Fund of the Chinese Academy of Sciences, from the State Science and Technology Commission of China, and from the Natural Science Foundation of China is gratefully acknowledged. The authors also express their appreciation to the State Council of China for providing a National Research Grant for Outstanding Young Scientists (No. 59525307).

REFERENCES

1. K. S. Minsker, U. V. Lisitsky, S. V. Kolesov, and G. E. Zaikov, *J. Macromol. Sci. Rev. Macromol. Chem.,* **C20,** 243 (1981).
2. J. A. Manson, *Pure Appl. Chem.,* **53,** 471 (1981).
3. G. H. Hofmann, in *Polymer Blends and Mixtures,* D. J. Walsh, J. S. Higgins, and A. Maconnachie, Eds., Martinus Nijhoff Publishers, Dordrecht, 1985.
4. M. K. Naqvi, *J. Macromol. Sci. Rev. Macromol. Chem. Phys.,* **C27,** 559 (1987).
5. A. A. Yassin and M. W. Sabaa, *J. Macromol. Sci. Rev. Macromol. Chem. Phys.,* **C30,** 491 (1990).
6. L. Nass, *Encyclopedia of PVC,* Marcel Dekker, New York, 1977, Vol. 2.
7. R. Deanin and N. Shah, *Org. Coat. Plast. Chem.,* **45,** 290 (1981).
8. G. Scott and M. Tahani, *Eur. Polym. J.,* **13,** 969 (1977).
9. V. I. Mandrukova and A. V. Stalbovskaya, *Stroit. Mater.,* **4,** 1977, (CA, 87:70328).
10. H. Masayanaki and S. Masato, Jpn. Kokai Koho 60, 155247 (1985) (to Denki Kagaku Kogyo).
11. S. N. Maiti, U. K. Saroop, and A. Misra, *Polym. Eng. Sci.,* **32,** 27 (1992).
12. R. P. Petrich, *Polym. Eng. Sci.,* **13,** 248 (1973).
13. A. M. Pavan, T. Ricco, and M. Rink, *Mater. Sci. Eng.,* **48,** 9 (1981).
14. S. I. Moroz and A. Varishtein, *Plast. Massay,* **1,** 15 (1983).
15. J. Brandrup and E. H. Immergut, *Polymer Handbook,* Wiley–Interscience, New York, 1975.
16. T. Nobuyuki, Japan. Kokai, 73 68642, 1973, (CA, 80:15787) (to Showa Denko K. K.).
17. N. Junichi and O. Masao, Jpn. Kokai 74 02848, 74 02849, 1974, (CA, 81:14309, 81:14310) (to Showa Denko K. K.).
18. Z. Zhong, S. Zheng, K. Yang, and Q. Guo, *J. Macromol. Sci. Phys.,* to appear.
19. N. G. McCrum, B. E. Read, and G. Williams, *Anelastic and Dielectric Effects in Polymeric Solids,* Wiley, New York, 1967.
20. G. Pezzin, G. Ajroldi, and C. Garbuglio, *J. Appl. Polym. Sci.,* **11,** 2553 (1967).
21. R. F. Boyer, *Polym. Eng. Sci.,* **8,** 161 (1968).
22. S. Havriliak, Jr. and T. J. Shortridge, *J. Vinyl Tech.,* **10,** 127 (1988).
23. S. Havriliak, Jr. and C. S. Pogonowski, *Macromolecules,* **22,** 2466 (1989).
24. Q. Guo, J. Huang, T. Chen, H. Zhang, Y. Yang, C. Hou, and Z. Feng, *Polym. Eng. Sci.,* **30,** 44 (1990).
25. Q. Guo, J. Huang, B. Li, T. Chen, H. Zhang, and Z. Feng, *Polymer,* **32,** 58 (1991).
26. Q. Guo, L. Qiu, M. Ding, and Z. Feng, *Eur. Polym. J.,* **28,** 481 (1992).
27. Q. Guo, L. Qiu, M. Ding, and Z. Feng, *Eur. Polym. J.,* **28,** 1045 (1992).
28. W. Liu, Q. Guo, and Z. Feng, *J. Appl. Polym. Sci.,* **46,** 1645 (1992).